CFD and experimental approaches to investigate a dynamic filtration module for bio- and food-processes - Approches expérimentale et numérique d'un module de filtration dynamique dédié aux procédés alimentaire et biotechnologique.

Morgane d' Esparbes, Philippe Schmitz, Luc Fillaudeau

Récents Progrès en Génie des Procédés, Numéro 101 - 2011
ISSN 1775-335X - ISBN 2-910239-75-6, Ed. SFGP, Paris, France

CFD and experimental approaches to investigate a dynamic filtration module for bio- and food-processes

Approches expérimentale et numérique d'un module de filtration dynamique dédié aux procédés alimentaire et biotechnologique

D'Esparbes M.[a], Schmitz Ph.[a], Fillaudeau L.[a*]

[a]Université de Toulouse, INSA, UPS, INPT, LISBP, 135 Av. de Rangueil, F-31077 Toulouse, France
INRA, UMR792 Ingénierie des Systèmes Biologiques et des Procédés, F-31400 Toulouse, France
CNRS, UMR5504, F-31400 Toulouse, France

Résumé

L'investigation de l'hydrodynamique d'un module de filtration dynamique, dénommé Rotating and Vibrating Filtration (technologie RVF), conçu pour le traitement de fluides biologiques et alimentaires, a été conduite à partir d'expérimentations pilote et de simulation numérique. Le module RVF (surface filtrante 0,048m2) se divise en deux chambres de filtration accueillant chacune deux membranes, fixées sur un support poreux, qui drainent le perméat. Un dispositif mécanique simple et en fonctionnement continu (jusqu'à 50Hz) permet de maintenir une contrainte de cisaillement élevée ainsi qu'une perturbation de la couche limite hydrodynamique sur les membranes. Le présent article se focalise sur le régime turbulent. Les champs de pression statique et de vitesse, obtenus numériquement, permettent d'analyser les vitesses locales et la force motrice de perméation. Les résultats, interprétés en termes de distribution radiale de pression et coefficient d'entraînement, sont qualitativement en accord avec l'expérience. Des variations temporelles de vitesse et de pression très importantes sont mises en évidence selon la position radiale en fonction de la vitesse de rotation. Nous pouvons ainsi expliquer les bonnes performances de filtration de cette technologie, par des interruptions périodiques de la pression transmembranaire associées à la génération d'instationnarités analogue à un écoulement pulsé.

Abstract

Laboratory experiments and CFD simulation have been performed to investigate hydrodynamics of a dynamic filtration technology, called Rotating and Vibrating Filtration (RVF technology) designed to treat biological suspensions. The RVF module (filtration area 0.048 m²) is divided into cells in series. Each cell includes two flat disc membranes fixed onto porous substrates which drain the permeate, and three blades impeller-shaped rotating bodies attached to a central shaft. This simple mechanical device runs continuously (up to 50Hz) and maintains a high shear rate as well as an unstationary hydrodynamics at the membrane surface. The present paper focuses on turbulent flow regime. Static pressure and velocity fields (CFD) are reported and indicate local velocity and permeation driving force. CFD and experimental measurements (radial pressure distribution, core velocity coefficient) with model fluids are qualitatively in agreement. Velocity and static pressure fields show drastic magnitude time variations with rotational speed and radial position. Filtration performances are explained by periodic interruption of transmembrane pressure associated to unstationarity generation equivalent to pulsed flow.

Mots-clés : filtration dynamique, hydrodynamique, experimentation, simulation numérique

Key-words: dynamic filtration, hydrodynamics, experiment, CFD.

[*] Auteur/s à qui la correspondance devrait être adressée : luc.fillaudeau@insa-toulouse.fr

1. Introduction

Membrane separation technology has become widely used in the food and bioprocess industry (biotechnology, dairy, juice, wine, water) (Cheryan, 1998; Daufin et al., 2001). For the membrane process, the choice of means of filtration (dead-end, cross-flow or dynamic filtration) and membranes (chemical nature, mean pore diameter) are crucial. Retention could be described by mechanical and or physico-chemical retention but the mechanisms of retention result from a complex balance between the nature and structure of membranes, the local hydrodynamic conditions and the product. In CFMF and dynamic, a dynamic selective layer (particle in suspension, macromolecules, and complex) is created and plays an important role in retention mechanism. The propensity of retention, the contribution of the different mechanisms, how they interplay on soluble and insoluble fractions, the quantification and characterization of fouling are investigated. In conventional cross-flow filtration, high tangential fluid velocities are generally necessary to limit the growth of cake on the membrane. These high velocities require energy and produce large pressure drops along the membrane. Consequently the transmembrane pressure remains high at membrane inlet, and this may limit solute transmission into the permeate when the cake layer on the membrane is compressible and is packed by pressure.

Dynamic filtration, which consists of creating relative motion between the membrane and its housing, avoids this problem, since high shear rate produced by the relative motion are independent of the feed flow, which can be kept low. In cross-flow filtration, the aim is to reduce the impact of fouling. A large number of hydrodynamic techniques, based on fluid instabilities, have been investigated such as co-current mode, pulsating flow, periodic stop of the transmembrane pressure, periodic back-flush or a back-shock process, generation of Dean or Taylor vortices, introduction of turbulence promoters (baffled channel, stamped membrane) or the use of a two-phase flow (gas–liquid, liquid–solid). In order to improve performances and to increase shear rate, new systems called dynamic filtration systems have been studied in food and biotechnological applications over the last decade. The specificity of dynamic filtration is that a mechanical device has been introduced in order to promote turbulence at membrane surface independently of retentate flow-rate. Dynamic filtration modules could use either a vibrating (Schneider et al., 2001) and rotating membrane (Serra et al. 1999), or the motion of a mechanical device with a rotating (Jaffrin, 2008) and/or vibration disc or impeller (Ermolaev et al., 2002) close to the membrane surface. Several dynamic filtration devices have been reported by manufacturer: Artisan (Artisan Industries), cross-rotational flow (ABB-Flootek), centrifugal membrane filtration (Spintek), cross-rotational membrane filtration (Komline-Sanderson), Hitachi (Hitachi), dynamic membrane filter and vibrating membrane filter (Pall society).

Laboratory experiments and CFD simulations have been performed to investigate hydrodynamics of a dynamic filtration technology, called Rotating and Vibrating Filtration (RVF technology) designed to treat biological suspensions. Global theoretical analysis and literature overview highlight that the local variables (shear rate, velocity and pressure) could not be easily estimated in the RVF module. CFD simulation enables to gain insight in the complex hydrodynamics fields and to explain fouling resistance reduction with food and biological fluids. Both laminar and turbulent flow regimes were investigated after preliminary mesh optimisation and best choice of initial and boundary conditions.

In present paper, our discussions focus on turbulent flow regime. Static pressure and velocity fields (CFD) are reported and indicate local velocity and permeation driving force. CFD and experimental measurements (radial pressure distribution, core velocity coefficient) with model fluids are qualitatively in agreement. Velocity and static pressure fields show drastic magnitude time variations with rotational speed and radial position. Filtration performances are explained by periodic interruption of transmembrane pressure associated to unstationarity generation equivalent to pulsed flow.

2. Materials & Methods

2.1 Experimental fluids and set-up

The RVF laboratory module (filtration area 0.048m²) is divided into two parallel cells including two flat disc membranes fixed onto porous substrates which drain the permeate, and impeller-shaped rotating bodies attached to a central shaft (Fillaudeau et al., 2007). This simple mechanical device runs

continuously and maintains a high shear rate as well as a hydrodynamic perturbation at the membrane surface. The impeller is made of three blades ($\varnothing_{ext}$=142mm, thickness=8mm) included in a horizontal plane between two membranes. The dimensions of cell housing are 14mm in height and 143mm in diameter. The gap between the blade and the membrane is small and equal to 3 mm. Transmembrane pressure (up to 300kPa) and rotational frequency (up to 50Hz) can be adjusted to reach the optimal conditions for filtration. The two separated cells make it possible to work with two different membranes in similar conditions. The membranes were flat discs with an external diameter of 142mm and a thickness of 0.25mm. Filtration area per membrane is equal to 0.012m² and forms a crown shape with an internal diameter of 62.25mm and an external diameter of 135.5mm (including corrections due to the gasket). The determination of hydrodynamic performances (radial pressure distribution, core velocity coefficient) was carried out with water (softened water filtered through three cartridges: activated carbon, 0.20 and 0.50µm) by measuring the flux versus radial permeable crowns (25<r<68mm, $dr=r_{i+1}-r_i$=5mm, i=0–8, and $r_{10}-r_9$=3mm) on the membrane (organic membrane PVC,2 µm) and impeller velocity (Fig. 3).

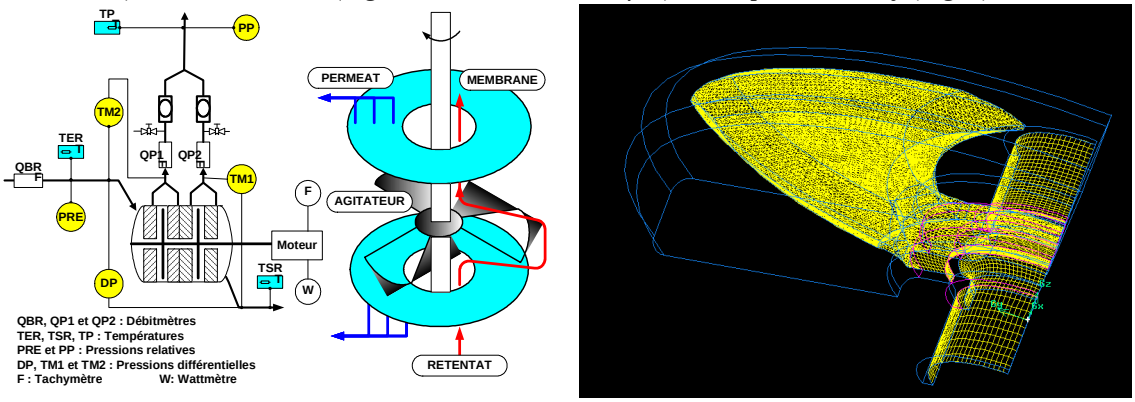

Figure 1. Schematic flow diagram of the RVF module with its instrumentation and impeller surface meshing (CFD).

2.2 CFD Model

We are especially interested in computing the turbulent flow in a unit filter element of the RVF module which consists of one cassette (Fig 1). We thus assume that each filter element works identically. While subsequent periodic boundary conditions at both ends can be reasonably assumed in laminar regime, they are questionable in turbulent regime. Therefore velocity pressure conditions at the inlet and outlet, respectively, are preferred, meaning that we consider a single cassette. Moreover angular periodic boundary conditions, which seem to be natural due to the particular geometry of the impeller (3 blades), need also to be discussed in turbulent regime. Thus two geometrical domains are studied: 120° (with angular periodic boundary conditions) and 360° domains. Finally we study the fluid flow in a rotating frame at the speed of the impeller. We consider the standard k-ε model for the fluid flow derived from incompressible Navier Stokes equations (Launder and Spalding, 1974). The corresponding governing equations and associated boundary conditions are expressed in cylindrical coordinates and solved using Gambit for meshing and Fluent software (ANSYS, 2006). Furthermore we assume that the flow is isothermal, i.e. the thermo-physical properties of the fluid remain constant.

It can be seen in fig 1 that the geometrical domain is complex. The associated flow is also expected to be complex, i.e. the main flow direction is difficult to anticipate. Indeed either in the annular ends region or past the impeller, the fluid velocity components will depend on one relevant parameter of the RVF module which is the rotation speed, N. Therefore we build a triangular meshing instead of a quadrangular meshing (less memory consuming). In addition, the maximum size of an elementary mesh is fixed at 1 mm. To take into account the expected high velocity gradients at the walls we impose a progressive refinement of the mesh size up to 0.17 mm at the walls. The resulting meshing used in the whole simulations consists of about 1,000,000 meshes. It is obtained from preliminary computations using 4 different meshes from 270,000 to 1,300,000 elementary meshes in which results are compared in terms of macroscopic values such as overall pressure drop and net viscous dissipation. We assume the convergence of the calculations when the residuals become lower than 10^{-6}.

3. Results

3.1 Experiments

The flow field between a static membrane and a rotating flat disk has been extensively studied as reported by Tu, 2009. The fluid flow encountered in this kind of confined dynamic filtration module is highly three-dimensional and axisymmetrical. Numerical calculations of the flow field between two infinite disks show that the boundary layers that develop both on the rotating and on the stationary disks could have different thicknesses. These various flow regimes have been identified as a function of geometrical and operating (flow-rate, mixing) conditions. The centrifugal force generates a radial outward flow near the rotating disk, which gives rise to an inward radial flow near the static membrane. The boundary layers are separated by an inviscid fluid core region which rotates at an angular velocity, ($k_{RD}.2.\pi.N$) with a core velocity coefficient inferior to 1.The core velocity coefficient depends on the disk geometry and on the membrane to disk gap. The radial pressure gradient in the boundary layer is equal to that in the inviscid core and is given by:

$$\frac{\partial p}{\partial r} = \rho \cdot r \cdot \left(k_{RD} \cdot 2 \cdot \pi \cdot N\right)^2 \qquad (1)$$

The pressure, uniform whatever the angular position, is obtained by integration of Eq.1 over membrane area from 0 to r assuming that k_{RD} is independent of the radius:

$$p(r) = 2 \cdot \rho \cdot \left(k_{RD} \cdot \pi \cdot N\right)^2 \cdot r^2 + p_0 \qquad (2)$$

In the RVF module, the flow field between the membrane and the rotating flat impeller is necessary different from a rotating flat disk system. The impeller induces high local variations related to rotational frequency of the impeller. Identically, the pressure varies along the angular position at time t. Analogous to the rotating flat disk system, we assume that the mean pressure $\langle p(r) \rangle_\theta$ at a given radius position can be derived from Eq.1 defining a core velocity coefficient, k_{RI} between the impeller and the membrane. The additional mean pressure $\langle p(r) \rangle_\theta - p_0$ was measured using an indirect method. Let us consider a membrane with a narrow permeable crown of width Δr at r position.

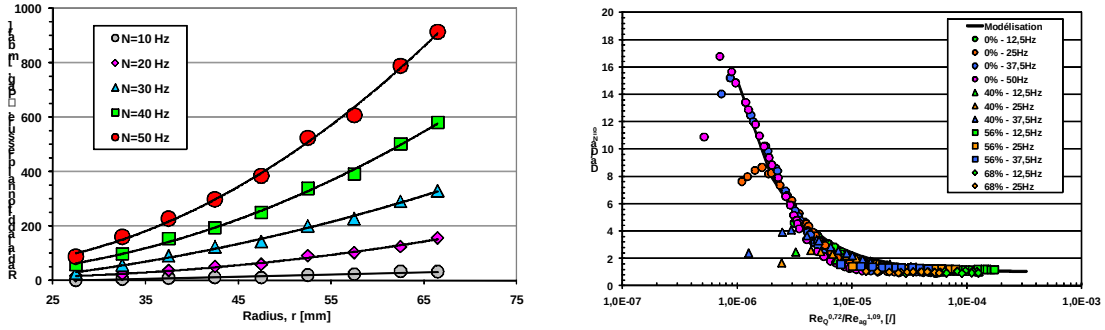

Figure 2. Determination of hydrodynamic performances, evolution of the radial pressure distribution versus the radius and the rotational speed and semi-empirical friction curve, $Da/Da_{N=0}$ versus $Re^{0,72}/Re_{ag}^{1,09}$.

The additional mean pressure at r position and rotation frequency N can be derived from Darcy's law, measuring the permeate flux with and without impeller rotation. It can be seen from Figure 2 that the quadratic variations of $\langle p(r) \rangle_\theta - p_0$ as a function of *r* and *N* are well verified. Thus the effect of the impeller velocity on the additional mean pressure is correctly described by Eq.2, taking k_{RI} = 0.62 (R^2=0.988) and 0<N<50rd/s. The core velocity coefficient exhibits a high value due to the specificity of the RVF module (narrow gap, impeller with 3 flat blades).

The lack of reliable models to describe the hydrodynamic parameter (pressure drop, power consumption) of the RVF module led us to make the following consideration: the RVF module can be compared to (1) a pipe of complex section in which circulates a Newtonian fluid and (2) a stirred mixing tank with a power and a permanent withdrawal. For model system 1, we do not know which criteria is needed to define the characteristic dimensions (*dh, S, L*), or the impact of the rotation speed of the impeller on the net pressure

drop per unit length. For model system 2, the influence of feed rate of the fluid on the power consumption, which also depends on the speed of rotation, remains to be determined. These two analogies are characterized by relationships between dimensionless numbers in laminar flow (theoretical system), experimental measurements (pressure drop, power consumption) led to identify dimensionless geometric criteria *(ξ, Kp*). The friction and the power consumption curves in the RVF module were reported by Fillaudeau et al., 2007. However, the investigation of local hydrodynamic is required to better understand the performances of the system. RVF technology stands as a complex device from a hydrodynamic point of view, making difficult to access to the local flow field from existing models, more specifically the mean shear rate and pressure as well as their local variations. Consequently, two additional approaches may be considered to bring new insight in hydrodynamic understanding: (i) Particle Image Velocimetry (PIV) and (ii) Computational Fluid Dynamics (CFD). PIV approach will constitute an alternative experiment but will require designing of a complex and transparent module for optical measurement. Numerical approach (CFD) enables us to directly obtain local information and to compare trends and computation results with experimental data.

3.2 CFD Model

CFD enables to determine pressure and velocity fields within the whole module. Presented results are limited to a rotational frequency of 25Hz, with water and 100l/h. Our discussion will focus on cassette region corresponding to the filtration area even if useful information may be extract for inlet and outlet area. Identically, the wall shear rate along the filtration surface will not be presented whereas it constitutes an important parameter to explain filtration performances.

3.2.1 Static pressure.

Figures 3 depict the static pressure profiles as a function of angular position for several radii (*r*=30, 40, 50 and 60mm) and different z-planes close to membrane (*z*=0.1mm) and impeller (*z*=2.9mm).

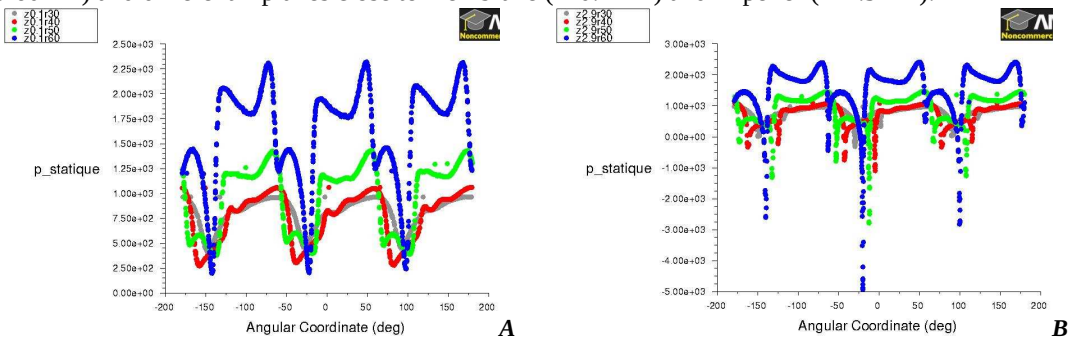

Figure 3. Static pressure versus angular coordinate (360°), radii (30, 40, 50 and 60mm) and z-plan positions (0.1 and 2.9mm)

Global overview shows the periodic impact of impeller, corresponding to three sharp peaks of mean static pressure followed by a plateau. Their magnitude is correlated with radial position, and the angle covered by the plateau with the geometry of the blade. It can be noticed that 360° simulation demonstrates the periodicity of flow, which validates 120° model including angular periodic boundary conditions.

Leading and trailing edges are easily identified on each curve. Mean static pressures sharply decrease behind the impeller, their values are close to zero at membrane surface and maybe negative in blade plane neighbourhood. The subsequent periodic transmembrane pressure is probably one of the effects responsible for good performance of this filtration process. The increase of rotational frequency induces an increase of these phenomena (results not presented).

3.2.2 Velocity fields

Figures 4-A and B illustrate the velocity magnitude fields for two different z-planes (z=0.1 and 2.9mm). Blade geometry is perfectly visible in figure 4-B (green to red colours). At membrane surface, mean velocity magnitude increases as a function of radial position, and exhibits high variations with angular position for a given radius according to blade position and geometry. As expected, the mean velocity magnitude increases under the blade associated with the reduction of the gap.

Mean static pressure and velocity magnitude are synchronised as both results indicate that pressure and velocity achieve minimum values between blades and maximum under the blades. Velocity field indicates that a maximum velocity (related to wall shear rate) and strong variations (unstationary flow) are correlated to impeller rotational frequency. Both mechanisms are expected to highly favour filtration performances. The core velocity coefficient, k_{RI} between the impeller and the membrane may be deduced from static pressure field. Contrary to model depicted in Eq.2 and experimental measurements (fig.2), CFD results show that k_{RI} depends on r (for r<45mm). A constant value k_{RI}=0.26 can be estimated when r>45mm which is significantly different as k_{RI}=0.62 (R^2 = 0.988) obtained from experimental measurements. This difference could be attributed to gaps between experimental and simulation parameters (operating conditions, geometrical characteristics) and/or to the choice of turbulence model.

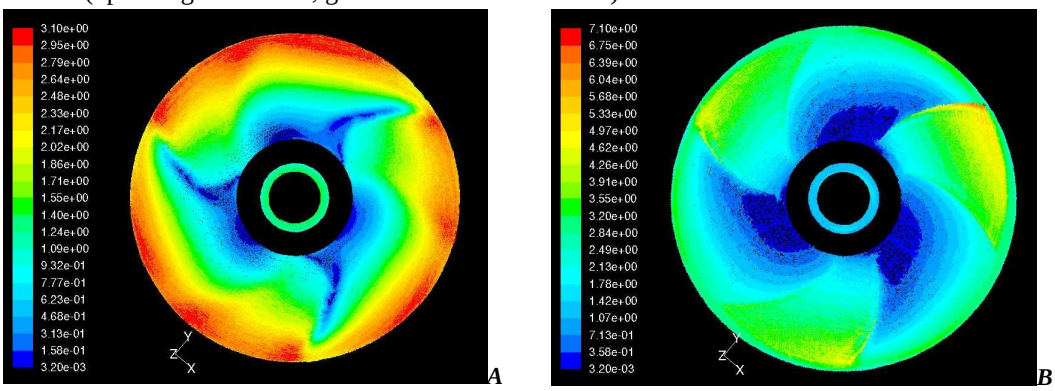

Figure 4. Velocity magnitude (m/s) versus z-planes (z=0.1 and 2.9mm).

4. Conclusion

The present paper reports the first CFD investigation of a complex dynamic filtration device focussing on turbulent flow regime. Static pressure and velocity fields were carefully examined. CFD and experimental measurements (radial pressure distribution, core velocity coefficient) with model fluids remain qualitatively in agreement. Filtration performances can be clearly explained by periodic interruption of transmembrane pressure associated to unstationary flow equivalent to pulsed flow. Numerical approach (CFD) enables us to directly obtain local information and to compare trends and computation results with experimental data. This information will be useful to calculate local and average shear rates in relation with structuring and destructuring of food and biological matrices. Moreover local and periodical unstationary flow is also expected to manage biological activity in bioprocesses. In the future, an alternative approach based on Particle Image Velocimetry (PIV) experiment could be used to merge and compare experimental and numerical investigations.

Références

Cheryan, M., 1998, Lancaster PN, USA, Technomic publishing Company, 349- 484.
Daufin G., J.P. Escudier, H. Carrère, S. Bérot, L. Fillaudeau, M. Decloux, 2001, TransIChemE 79 Part A, 1-14.
Ermolaev S., L. Fillaudeau, G. Ricatte, A. Moreau, N. Jitariouk, A. Gourdon, 2002, 7ème coll PROSETIA, Compiègne, France, 36-41.
Fillaudeau L., B. Boissier, S. Ermolaev, N. Jitariouk, A. Gourdon, 2007, Ind. Alim. Agri. 124(9), 8-16.
Fillaudeau L., B. Boissier, A. Moreau, P. Blanpain-Avet, S. Ermolaev, N. Jitariouk, A. Gourdon, 2007, J. Food Eng, 80, 206-217.
Jaffrin M., 2008, J. Mem. Sci., 324, 7-25.
Launder B. E., D. B. Spalding, 1974, Comp. Methods Applied Mech. and Eng. 3(2), 269-289.
Murkes J., C.G. Carlsson, 1988, Ed. John Wiley & Sons, New York.
Schneider J., M. Krottenthaler, W. Back, H. Weisser, 2001, In: 28th Congress of EBC, Budapest, Hungary.
Serra C.A., M.R. Wiesner, J.M. Lainé, 1999, Chem. Eng. J. 72, 1-17.
Tu Z., 2009, PhD Thesis UTC, Compiègne, France.